Eur Radiol (2010) 20: 2882–2889
DOI 10.1007/s00330-010-1866-8

Sven F. Thieme
Sandra Hoegl
Konstantin Nikolaou
Juergen Fisahn
Michael Irlbeck
Daniel Maxien
Maximilian F. Reiser
Christoph R. Becker
Thorsten R. C. Johnson

Pulmonary ventilation and perfusion imaging with dual-energy CT

Received: 20 January 2010
Revised: 13 May 2010
Accepted: 21 May 2010
Published online: 23 June 2010

S. F. Thieme · K. Nikolaou · D. Maxien · M. F. Reiser · C. R. Becker · T. R. C. Johnson
Department of Clinical Radiology, Ludwig Maximilians University, Klinikum Großhadern, Marchioninistr. 15, 81377, München, Germany

S. Hoegl · J. Fisahn · M. Irlbeck
Department of Anesthesiology, Ludwig Maximilians University, Klinikum Großhadern, Marchioninistr. 15, 81377, München, Germany

S. F. Thieme (✉)
Institut für Klinische Radiologie der LMU München,
Klinikum Großhadern,
Marchioninistr. 15, 81377, München,
Germany
e-mail: sven.thieme@med.lmu.de
Tel.: +49-89-70953620

Abstract *Objective* To evaluate the feasibility of dual-energy CT (DECT) ventilation imaging in combination with DE perfusion mapping for a comprehensive assessment of ventilation, perfusion, morphology and structure of the pulmonary parenchyma. *Methods* Two dual-energy CT acquisitions for xenon-enhanced ventilation and iodine-enhanced perfusion mapping were performed in patients under artificial respiration. Parenchymal xenon and iodine distribution were mapped and correlated with structural or vascular abnormalities. *Results* In all datasets, image quality was sufficient for a comprehensive image reading of the pulmonary CTA images, lung window images and pulmonary functional parameter maps and led to expedient results in each patient. *Conclusion* With dual-source CT systems, DECT of the lung with iodine or xenon administration is technically feasible and makes it possible to depict the regional iodine or xenon distribution representing the local perfusion and ventilation.

Keywords Dual-energy CT · Lung ventilation CT · Functional lung imaging · Dual-energy functional pulmonary CT · Xenon ventilation CT

Introduction

Whenever high-resolution morphological information on structural changes of the lung parenchyma is needed, CT is the first-line imaging technique, applying so-called high-resolution (HR) protocols with a narrow reconstructed slice thickness and a high-resolution reconstruction algorithm. In the field of functional lung imaging, dual-energy CT (DECT) using dual-source CT (DSCT) systems with two independent tube–detector units makes improved material differentiation feasible [1]. Previous studies have shown that DECT can map the iodine distribution in the lung parenchyma and detect perfusion changes or defects [2–7]. Thus, DECT is able to combine morphological and functional lung imaging.

The inert gas xenon (Xe) has X-ray absorption characteristics that resemble those of iodine, so it can serve as an inhalant contrast agent for CT ventilation imaging. Although there have been trials in previous decades using stable xenon gas for CT ventilation imaging, this method had not been used in clinical care. These previous approaches were based on sequential acquisitions, implying an increased patient dose and potential misregistrations due to varying levels of inspiration [8–13]. With dual-source CT systems that can acquire two spiral CT datasets with different photon spectra simultaneously, DECT now has the potential to map xenon distribution patterns by directly visualising the inhaled xenon gas. Chae et al. performed xenon-enhanced DECT in 12 subjects at an inspiratory xenon concentration

Table 1 Demographic data, clinical history and abnormal morphological findings

Pat ID	Age (years)	Sex	Clinical history	Ventilation parameters (MV; f; ppeak; PEEP; I/E)	Xenon consumption (l)	Lung windows	CTA/soft tissue findings
1	57	M	Bilateral lung transplantation	9.9; 10; 20; 3; 1:2	4.92	Right pneumothorax; left pleural effusion and atelectasis of segments 9 and 10	No abnormal findings
2	65	M	Single (left) lung transplantation	7.0; 12; 24; 5; 1:2	3.02	Right bullous emphysema; left pneumothorax and lower lobe atelectasis in graft	No abnormal findings
3	67	F	Single (right) lung transplantation	5.0; 17; 28; 5; 1:1	2.86	Left fibrosis (reticular pattern, cysts); right bronchiectasis (segments 9 and 10) in graft	Pericardial effusion
4	40	F	ARDS following pneumonia	7.0; 15; 24; 17; 1:1	2.47	Diffuse GGOs and consolidations	No abnormal findings
5	71	M	Previous ARDS following pneumonia	8.0; 12; 25; 8; 1:2	2.96	Severe fibrosis with lung volume loss	Enlargement of central pulmonary arteries, pulmonary trunk 3.4 cm
6	56	F	Aortic dissection	6.0; 12; 25; 3; 1:2	1.80	Congestion; oedema	Left ventricular enlargement; dissection of thoracic aorta; prosthetic replacement of ascending aorta
7	37	M	ARDS following bleomycin treatment	9.5; 30; 20; 8; 1:2	4.61	Pneumonic opacities; mediastinal emphysema	No abnormal findings
8	69	M	Septic shock; previous ARDS	8.0; 14; 27; 13; 1:2	1.70	Minor infiltration and atelectases	No abnormal findings
9	49	F	Gastric cancer; gastrectomy	8.7; 10; 20; 3; 1:2	3.35	Bilateral apical bullous changes; left lower lobe atelectasis; right lower lobe segmental hypoattenuation (segments 9 and 10) with bronchiolitic changes	Soft tissue emphysema and mediastinal emphysema; left pleural effusion
10	60	F	Bilateral lung transplantation	5.0; 12; 24; 7; 1:2	3.26	Right basal pneumothorax	Rarefied subsegmental arteries n right upper lobe (segments 2 and 3)

M male, *F* female, *MV* respiratory minute volume (l/min), *f* respiratory rate (1/min), *ppeak* peak airway pressure (cmH_2O), *PEEP* positive end-expiratory pressure (cmH_2O), *I/E* inspiratory to expiratory time ratio, *CTA* CT angiography, *ARDS* acute respiratory distress syndrome, *GGOs* ground glass opacities

of 30% and showed the technical feasibility of DECT ventilation imaging [14].

As both ventilation and perfusion are crucial for adequate blood oxygenation, the aim of our study was to use dual-energy (DE) ventilation/perfusion imaging in patients with pulmonary functional impairment, i.e. deterioration of the gas exchange during intensive care treatment, to evaluate the technical feasibility of a comprehensive imaging method. As inhaled xenon can have anaesthetic properties in higher concentrations [15, 16], this initial study was performed in patients under long-term sedation in cooperation with the anaesthesiology department.

Materials and methods

Patients

The study was performed in ten patients (five male, five female; mean age, 57 years; range, 34–76 years) who were referred for CT imaging from the anaesthesiological intensive care units (ICU) of our hospital. Patient demographics and clinical history are reported in Table 1. All patients were under long-term sedation with endotracheal intubation and were ventilated artificially.

In all patients, chest CT examinations were requested by the referring physicians to evaluate the pulmonary parenchyma, existence or progression of pneumonia or acute respiratory distress syndrome (ARDS) as well as detection of pulmonary embolism during their intensive care treatment. The use of xenon as a CT contrast material had been approved by the institutional review board, and before sedation all patients or their legal guardians had given written informed consent to the examination including the use of xenon gas in the event of chest CT being necessary.

DECT examination

The first six consecutive patients were examined on a first-generation 64-slice dual-source CT (Somatom Definition DS, Siemens Healthcare, Forchheim, Germany). After installation of the successor system, four more examinations were performed on a second-generation 128-slice dual-source CT (Somatom Definition FLASH, Siemens Healthcare, Forchheim, Germany).

Patients were transferred to the radiology department under sedation, attended and monitored by an anaesthesiologist with continuous pulse oximetry during transport and examination. Mechanical ventilation settings from the ICU were not changed during transport and examination (Table 1). Immediately before CT, the respiration regimen was modified to inspiratory fractions of 50% oxygen and 50% stable xenon (Air Liquide, Düsseldorf, Germany). A dedicated closed respiration system (Tangens 2c, EKU Elektronik, Leiningen, Germany) was used. After connection to the ventilator, patients were ventilated with 100% oxygen for at least 5 min for proper denitrogenation. Then, automatic xenon dosing was activated and the wash-in phase was started. The expiratory xenon concentration was continuously monitored and CT was started at an expiratory xenon concentration of 30%. Xenon ventilation was continued during this first CT acquisition.

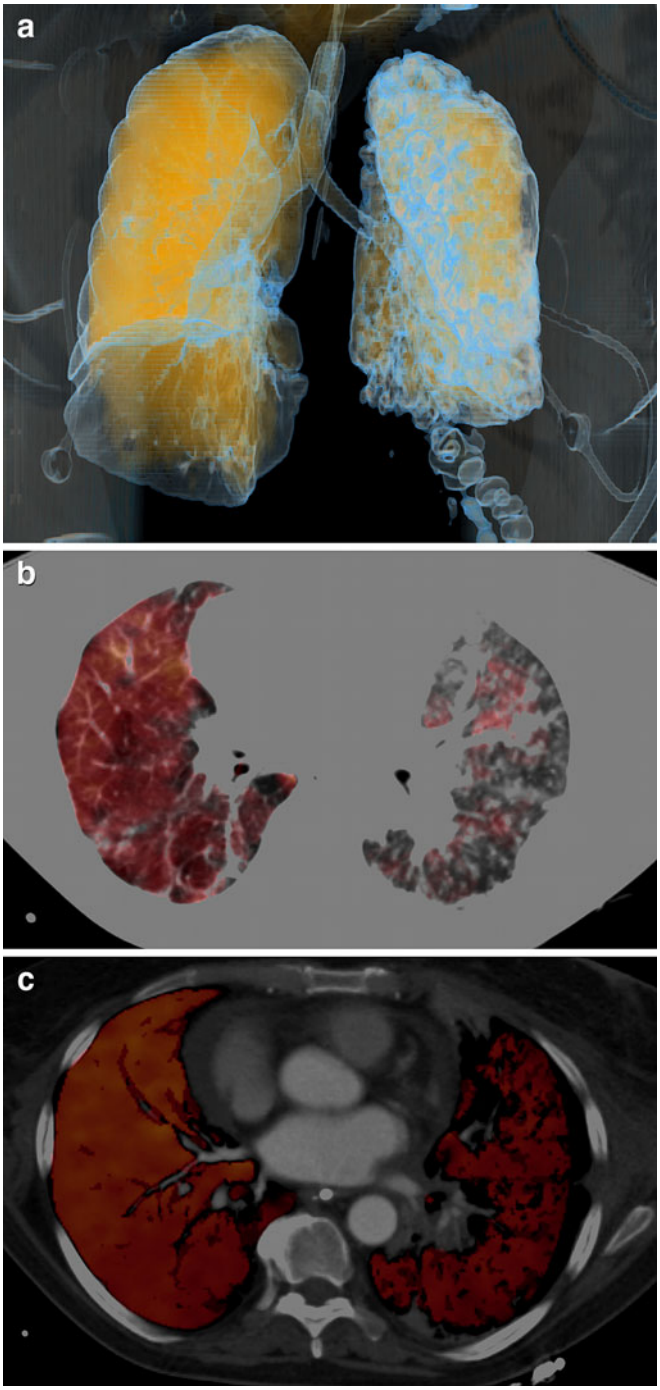

Fig. 1 A 67-year-old female patient (patient #3) with idiopathic pulmonary fibrosis after right lung transplantation. **a** Volume rendering technique with *yellow* display of xenon distribution; **b** axial fused image of lung window and colour-coded xenon map showing largely homogeneous ventilation of the right lung and volume loss with patchy hypoventilation of the fibrotic left lung; **c** fused soft tissue window and iodine map at the same level as in **a** showing homogeneous perfusion of the graft and slightly decreased perfusion with several defects in the left lung

For the first-generation DSCT examinations, acquisition parameters were: tube voltages, 140 and 80 kVp at 30 and 117 effective mAs with attenuation-based tube current modulation; rotation time, 0.5 s; collimation, 14×1.2 mm; pitch, 0.7. With the new features and technical improvements in the second-generation system, harder X-ray spectra with a filtered 140-kVp spectrum with a 0.1-mm tin filter and a 100-kVp lower-energy spectrum were applied. As these spectra provide improved general transmission with less noise, a thinner collimation of 128×0.6 mm could be used. Remaining parameters were: tube currents, 165 and 140 effective mAs with attenuation-based modulation; rotation time, 0.28 s; and pitch, 0.55. CT range included the whole lungs from apex to base. The tube currents had been adapted such that the CT dose index was identical at 5.37 mGy for both protocols. Mean examination time was 11.2 s for the 64-slice DSCT protocol and 8.7 s for the 128-slice DSCT protocol. After the ventilation CT acquisition, respiration parameters were switched to 100% oxygen and intravenous injection of contrast material (iopromide, Ultravist 370, Bayer Schering Pharma, Berlin, Germany) was initiated as soon as a threshold value of less than 5% expiratory xenon concentration was reached (3–5 min after the switch to 100% oxygen) in order to avoid a residual xenon-related X-ray attenuation on the iodine-enhanced images. Then 80 ml of contrast material was injected at 4.0 ml/s, followed by 100 ml saline. Perfusion DECT was acquired with identical parameters to the xenon-enhanced ventilation examination. Timing was optimised for the pulmonary parenchymal phase with a bolus tracking technique (threshold=100 Hounsfield units (HU in the pulmonary trunk, delay 7 s) [5]. Mechanical ventilation was not paused during CT.

Dose length products (DLP) were recorded from the patient protocols. For an estimation of the effective patient dose, the DLP was multiplied by a conversion factor of 0.017 mSv mGy^{-1} cm^{-1} [17].

Image reconstruction

Images were reconstructed separately from both simultaneous spiral acquisitions using specific soft kernels that do

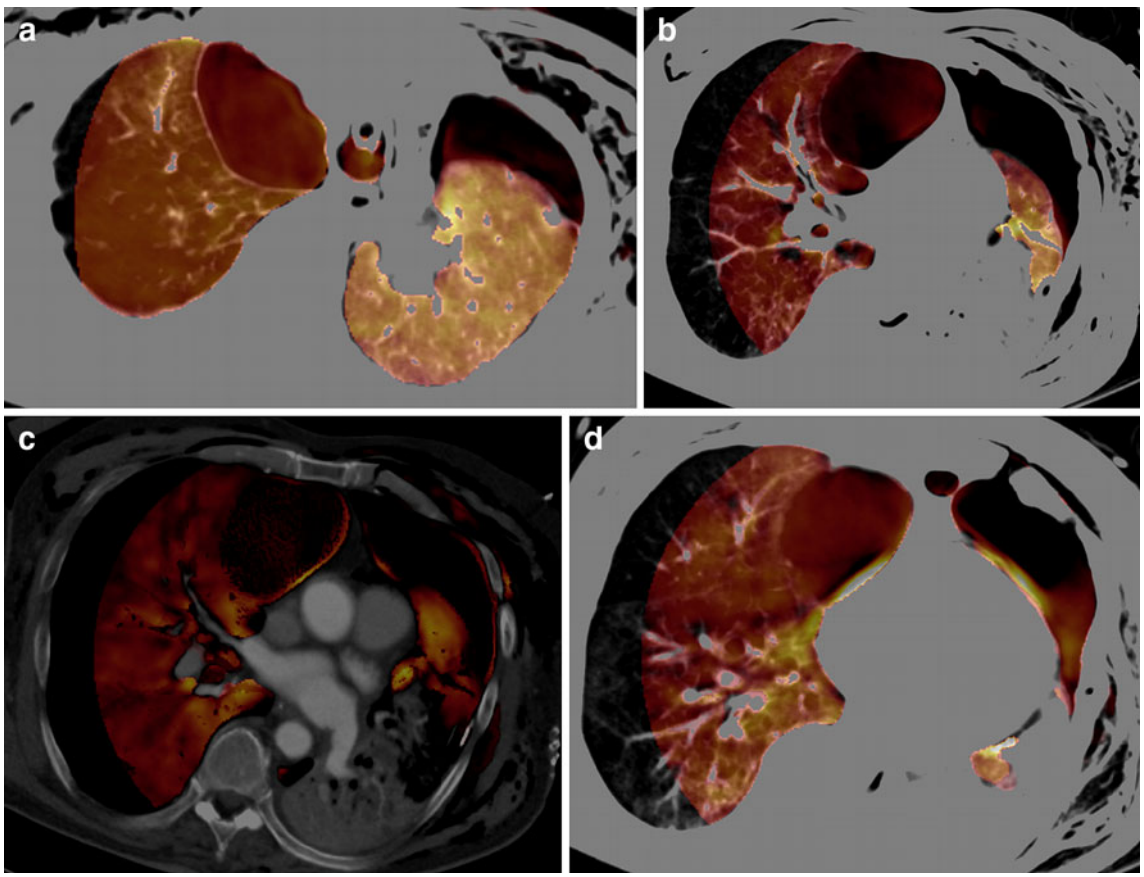

Fig. 2 A 65-year-old male patient (patient #2) with left lung transplantation. **a** Fused image of the lung window and the xenon map at a suprahilar level showing decreased ventilation of the emphysematous right lung with relative hyperventilation of the left-sided graft. An anteriorly located subpleural bulla in the right upper lobe shows xenon enhancement. Left pneumothorax and soft tissue emphysema are shown without xenon content. **b** Xenon and **c** iodine distribution maps show ventilation but no perfusion of the bulla. Little signal within the bulla in **c** is probably caused by residual xenon due to delayed ventilation of the bulla. **d** At a more caudal level, xenon enhancement within the pneumothorax indicates fistula of the visceral pleura. This finding was in accordance with a persistent partial collapse of the left lung in spite of chest tube therapy. As a result of the threshold levels of the DE algorithm, xenon/iodine distribution is not assessable in these dense atelectatic lung areas

not alter object edges (D20). In order to obtain an adequate signal to noise ratio (SNR), slice thickness was set to 3 mm, increment 1 mm. The resulting high (140 or tin-filtered 140 kVp) and low (80 or 100 kVp) image datasets were transferred to a post-processing workstation (Syngo Multi Modality Workplace, Siemens Healthcare, Forchheim, Germany). Colour-coded distribution maps of xenon and iodine were generated with specific DE post-processing software approved by the US Food and Drug Administration [1]. This software analyses the density values in the corresponding high- and low-energy CT datasets using a decomposition algorithm to quantify and visualise the photo effect caused by iodine or xenon. The parameters of the three-material decomposition were set to −1,000 HU for air at both photon energies, 60/56 HU at 80/100 kVp and 54/52 HU at 140/Sn140 kVp for soft tissue, a density between −960 and −600 HU, a slope of 2.00 for 140/80 kVp or 2.18 for 100/Sn140 kVp ("rel. CM" on the user panel) and an averaging ("range") over a radius of 4 voxels. As results, colour-coded ventilation and perfusion images (i.e. xenon and iodine distribution maps) were generated with a slab thickness of 3 mm. Additionally, weighted average images were calculated from both datasets using soft tissue (D30, soft kernel without edge alteration) as well as lung window (H70, edge enhancing hard convolution kernel) reconstruction algorithms at 1.5-mm slice thickness and 1.0-mm increments.

Data analysis

Image reading was performed by two radiologists in consensus with 7 and 3 years' experience in thoracic imaging. A ventilation or perfusion defect was recorded in areas that appeared substantially darker on the colour maps than on the surrounding areas. The following image interpretation criteria were employed:

(a) Reading of the ventilation maps, recording of ventilation heterogeneities by lung segment;
(b) Reading of the perfusion maps, likewise recording heterogeneities;
(c) Interpretation of the lung window images, recording parenchymal alterations and other abnormalities such as presence and extent of pleural effusion, pneumothorax or oedema;
(d) Analysis of the soft tissue images derived from the contrast-enhanced acquisition with pulmonary arterial

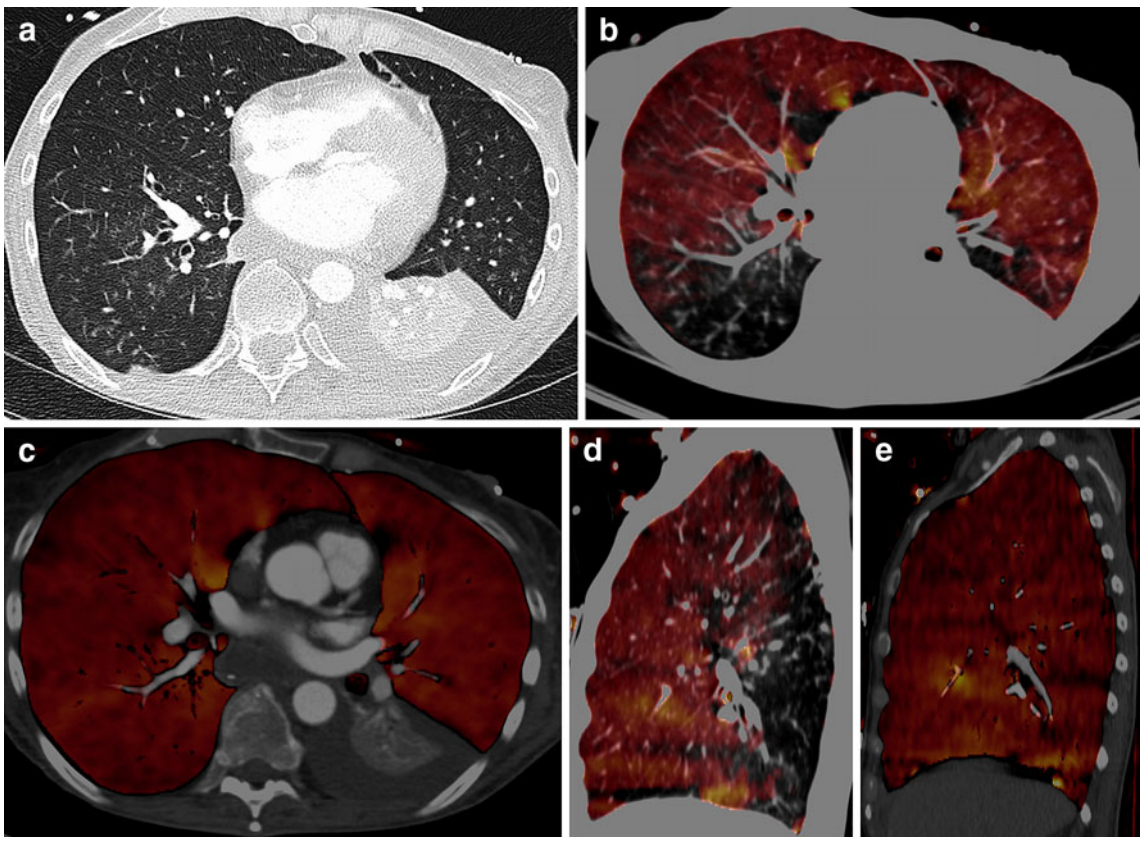

Fig. 3 A 49-year-old female patient (patient #9) with post-infectious bronchiolitis. **a** High-resolution lung window shows hypoattenuating lobules in the right lower lobe as well as small nodular opacities and branching tubular subpleural structures, consistent with bronchiolitis. **b** Axial and **d** sagittal xenon maps as well as **c** axial and **e** sagittal iodine maps show restricted ventilation in the right lower lobe corresponding to the area of bronchiolitis without perfusion defect. As a result of thresholding of the DE algorithm, xenon/iodine distribution is not assessable in the atelectatic left lower lobe

contrast enhancement, recording structural abnormalities of the heart and mediastinal structures and of the pulmonary vessels, also recording pulmonary embolism by lung segment, if present.

Findings of the ventilation and perfusion maps were classified as match (i.e. concordant ventilation and perfusion defects) or mismatch (i.e. differing patterns). Additionally, pathological or abnormal findings as depicted in the lung and soft tissue window setting correlated with abnormalities on the parameter maps.

Results

All examinations were successfully completed. No undesirable effects potentially related to xenon inhalation or intravenous contrast administration were observed during the examinations or during patient follow-up at the ICU where the patients were continuously monitored with pulse oximetry. The mean cumulative equivalent dose for both CT examinations was 9.38 mSv (standard deviation, 2.83 mSv). Mean xenon consumption per patient was 3.10 l (1.70–4.92 l, Table 1).

Despite some artefacts, mainly pseudo perfusion defects on the iodine maps due to beam hardening caused by dense contrast material in the vena cava or right heart, assessment of the parameter maps was not seriously hampered in any of the patients. In three of the six patients who were examined with the first-generation DSCT system, the peripheral parts of the dorsobasal lungs (up to 2.5 cm on each side) were not fully covered by the two X-ray tubes because of the smaller field of view (FoV) of the second detector (26 cm reconstructed FoV) (Figs. 1c, 2). On the successor system, the FoV of the second detector was large enough (33 cm) to completely cover both lungs in all patients (Fig. 3).

The findings of the xenon and iodine distribution maps corresponded well with morphological findings and matched the clinical diagnoses. A per patient synopsis of the results, including a diagnosis based on

Table 2 Findings of the functional parameter maps with xenon/iodine maps indicating ventilation/perfusion heterogeneities

Patient ID	Xenon map findings	Iodine map findings	Correlation of xenon/iodine findings	Diagnosis	Dose length product (mGy cm)	Equivalent dose (mSv)
1	Defect in left segments 9 and 10	No defects; slightly higher iodine content in dorsal parts	Mismatch	Ventilation deficits corresponding to morphological changes	228	3.88
2	Decreased ventilation of right lung; no defects in bullae; xenon enhancement in basal parts of pneumothorax	Defects corresponding to bullae. No corresponding defects in areas of decreased ventilation	Mismatch	Mismatching V/Q defects corresponding to respective morphological changes	690	11.73
3	Left: patchy pattern with multiple defects; right: homogeneous	Left: slightly patchy pattern; right: homogeneous	Mismatch	Fibrosis with functional impairment (V>Q); bronchiectasis in graft without functional impairment	597	10.15
4	Xenon mapping impossible in areas of consolidation; decreased ventilation in areas of GGOs	Iodine mapping impossible in areas of consolidation. No matching defects in areas of GGOs	Mismatch	ARDS with ventilation deficit	407	6.92
5	Multiple defects in both lungs	More homogeneous than xenon distribution; partially corresponding defects	Mismatch	Suspected PAH due to fibrosis. Consecutive functional impairment (V>Q)	695	11.92
6	Slightly reduced ventilation in dorsal parts of both lungs	Homogeneous distribution	Mismatch	Oedema with slightly reduced ventilation in dorsal parts	684	11.63
7	Multiple defects in both lungs	Defects corresponding to xenon maps, less pronounced	Match	ARDS with functional impairment	671	11.41
8	No defects; homogeneous distribution	No defects; homogeneous distribution	Match	Minor infiltration/ dystelectasis without relevant functional impairment	664	11.23
9	Right: segments 9 and 10	Apical defects corresponding to bullae	Mismatch	Air trapping in areas of bronchiolitis	366	6.22
10	No defects; homogeneous distribution	Right: defect in segments 2 and 3	Mismatch	Suspicion of peripheral PE	512	8.70

The functional imaging findings were correlated, and a diagnosis was made in consideration of functional and morphological findings. Dose length product and estimated equivalent dose represent the cumulative radiation dose of both scans

PE pulmonary embolism, *PAH* pulmonary arterial hypertension, *V/Q* ventilation/perfusion

morphological and functional imaging findings, is outlined in Table 2.

Discussion

In this study, we used DECT to obtain xenon and iodine maps that correspond to the functional parameters of ventilation and perfusion. In patients with abnormalities in lung structure and functional impairment, the combination of structural and functional information obtained from DECT might help in the follow-up during the course of the disease. The detection of lung areas exhibiting no substantial residual lung function could also assist the planning of lung volume reduction surgery in chronic obstructive pulmonary disease (COPD) patients. Also, the use of this technique can be helpful in the assessment of lung structure and function in critically ill patients with pulmonary functional impairment. Although ventilation and perfusion represent dynamic processes that would require multiple subsequent acquisitions for a complete assessment, the distribution of xenon and iodine during the wash-in phase of the respective agent should reveal heterogeneities compatible with defects in ventilation or perfusion. Assuming a monoexponential form of the wash-in curve of xenon [18] for non-diseased lung tissue, relatively short equilibration times of less than 2 min during the wash-in phase of xenon have been shown [10]. This means that an alveolar xenon concentration nearly equal to the inspiratory concentration is reached within this time period. Optimally, the time of acquisition should be tailored to the alveolar xenon concentration, i.e. imaging should be started as soon as an expiratory concentration of 30% is reached. Thus, an equilibration of xenon concentrations between areas of normal and restricted ventilation should be avoided. For perfusion imaging, the time of examination should match the "parenchymographic" contrast enhancement phase, in which functionally impaired areas are not yet opacified by iodine. Based on our own previous experience, a delay of 7 s is appropriate.

As we were able to show by means of the DLP, the individual DECT examinations do not result in an increased patient dose compared with conventional chest CT. Investigations using objective dose measurements with thermoluminescent detectors in Alderson phantoms have confirmed these observations [19]. However, at present, two entire DE acquisitions are required for a comprehensive assessment of ventilation and perfusion, as the selective visualisation of xenon and iodine is based on the photoelectric effect and the effects caused by those two elements cannot be separated into single acquisitions if both contrast agents are administered simultaneously.

The well-known anaesthetic properties of Xe in inspiratory concentrations exceeding 50–60% cause safety concerns regarding the use of this noble gas for diagnostic purposes. However, studies have shown that the rate of undesirable side effects is very low in inspiratory concentrations of 30% and less [20]. Chae et al. performed xenon-enhanced DECT in non-anaesthetised patients with 30% inspiratory concentration, yielding good results and observing few side effects [14]. With the new tin filter ('selective photon shield') integrated into the second-generation DSCT system, the improved spectral separation may make it feasible to work with lower xenon concentrations. Thus, future studies may be performed at lower xenon concentrations without sedation and without anaesthesiological patient monitoring. A decrease in total xenon dose per examination would also be desirable as xenon gas is rather expensive [21].

Conclusion

With dual-source CT systems, DECT of the lung with iodine or xenon administration is technically feasible and makes it possible to depict the regional iodine or xenon distribution. In our initial clinical experience, the resulting iodine and xenon maps seem to represent regional ventilation and perfusion and may serve as surrogates for V/Q scintigraphy. For the clinical use of xenon as an inhalant contrast agent, further studies are required especially with regard to a further reduction of the inhaled xenon concentration, and to prove the added diagnostic value of DECT over morphological CT or V/Q scintigraphy alone.

References

1. Johnson TR, Krauss B, Sedlmair M et al (2007) Material differentiation by dual energy CT: initial experience. Eur Radiol 17:1510–1517. doi:10.1007/s00330-006-0517-6
2. Thieme SF, Becker CR, Hacker M, Nikolaou K, Reiser MF, Johnson TR (2008) Dual energy CT for the assessment of lung perfusion–correlation to scintigraphy. Eur J Radiol 68:369–374
3. Pontana F, Faivre JB, Remy-Jardin M et al (2008) Lung perfusion with dual-energy multidetector-row CT (MDCT): feasibility for the evaluation of acute pulmonary embolism in 117 consecutive patients. Acad Radiol 15:1494–1504
4. Fink C, Johnson TR, Michaely HJ et al (2008) Dual-energy CT angiography of the lung in patients with suspected pulmonary embolism: initial results. Rofo 180:879–883
5. Thieme SF, Johnson TR, Lee C et al (2009) Dual-energy CT for the assessment of contrast material distribution in the pulmonary parenchyma. AJR Am J Roentgenol 193:144–149
6. Zhang LJ, Zhao YE, Wu SY et al (2009) Pulmonary embolism detection with dual-energy CT: experimental study of dual-source CT in rabbits. Radiology 252:61–70

7. Pansini V, Remy-Jardin M, Faivre JB et al (2009) Assessment of lobar perfusion in smokers according to the presence and severity of emphysema: preliminary experience with dual-energy CT angiography. Eur Radiol 19:2834–2843
8. Gur D, Drayer BP, Borovetz HS, Griffith BP, Hardesty RL, Wolfson SK (1979) Dynamic computed tomography of the lung: regional ventilation measurements. J Comput Assist Tomogr 3:749–753
9. Gur D, Shabason L, Borovetz HS et al (1981) Regional pulmonary ventilation measurements by xenon enhanced dynamic computed tomography: an update. J Comput Assist Tomogr 5:678–683
10. Murphy DM, Nicewicz JT, Zabbatino SM, Moore RA (1989) Local pulmonary ventilation using nonradioactive xenon-enhanced ultrafast computed tomography. Chest 96:799–804
11. Tajik JK, Chon D, Won C, Tran BQ, Hoffman EA (2002) Subsecond multisection CT of regional pulmonary ventilation. Acad Radiol 9:130–146
12. Simon BA (2005) Regional ventilation and lung mechanics using X-ray CT. Acad Radiol 12:1414–1422
13. Kreck TC, Krueger MA, Altemeier WA et al (2001) Determination of regional ventilation and perfusion in the lung using xenon and computed tomography. J Appl Physiol 91:1741–1749
14. Chae EJ, Seo JB, Goo HW et al (2008) Xenon ventilation CT with a dual-energy technique of dual-source CT: initial experience. Radiology 248:615–624
15. Rossaint R, Reyle-Hahn M, Schulte Am Esch J et al (2003) Multicenter randomized comparison of the efficacy and safety of xenon and isoflurane in patients undergoing elective surgery. Anesthesiology 98:6–13
16. Sanders RD, Franks NP, Maze M (2003) Xenon: no stranger to anaesthesia. Br J Anaesth 91:709–717
17. Huda W, Ogden KM, Khorasani MR (2008) Converting dose-length product to effective dose at CT. Radiology 248:995–1003
18. Kety SS (1951) The theory and applications of the exchange of inert gas at the lungs and tissues. Pharmacol Rev 3:1–41
19. Schenzle J, Sommer W, Neumaier K et al (2010) Dual energy CT of the chest - how about the dose? Invest Radiol. doi:10.1097/RLI.0b013e3181df901d
20. Latchaw RE, Yonas H, Pentheny SL, Gur D (1987) Adverse reactions to xenon-enhanced CT cerebral blood flow determination. Radiology 163:251–254
21. Hanne P, Marx T, Musati S, Santo M, Suwa K, Morita S (2001) Xenon: uptake and costs. Int Anesthesiol Clin 39:43–61